

University of Groningen

Paediatric cardiomyopathies

Herkert, Johanna Cornelia

DOI:
[10.33612/diss.97534698](https://doi.org/10.33612/diss.97534698)

IMPORTANT NOTE: You are advised to consult the publisher's version (publisher's PDF) if you wish to cite from it. Please check the document version below.

Document Version
Publisher's PDF, also known as Version of record

Publication date:
2019

[Link to publication in University of Groningen/UMCG research database](#)

Citation for published version (APA):
Herkert, J. C. (2019). *Paediatric cardiomyopathies: an evolving landscape of genetic aetiology and diagnostic applications*. Rijksuniversiteit Groningen. <https://doi.org/10.33612/diss.97534698>

Copyright

Other than for strictly personal use, it is not permitted to download or to forward/distribute the text or part of it without the consent of the author(s) and/or copyright holder(s), unless the work is under an open content license (like Creative Commons).

The publication may also be distributed here under the terms of Article 25fa of the Dutch Copyright Act, indicated by the "Taverne" license. More information can be found on the University of Groningen website: <https://www.rug.nl/library/open-access/self-archiving-pure/taverne-amendment>.

Take-down policy

If you believe that this document breaches copyright please contact us providing details, and we will remove access to the work immediately and investigate your claim.

Downloaded from the University of Groningen/UMCG research database (Pure): <http://www.rug.nl/research/portal>. For technical reasons the number of authors shown on this cover page is limited to 10 maximum.

Chapter 7

Biallelic truncating mutations in *ALPK3* cause severe paediatric cardiomyopathy

Rowida Almomani*, Judith M.A. Verhagen*, Johanna C. Herkert, Erwin Brosens, Karin Y. van Spaendonck-Zwarts, Angeliki Asimaki, Paul A. van der Zwaag, Ingrid M.E. Frohn-Mulder, Aida M. Bertoli-Avella, Ludolf G. Boven, Marjon A. van Slegtenhorst, Jasper J. van der Smagt, Wilfred F.J. van IJcken, Bert Timmer, Margriet van Stuijvenberg, Rob M. Verdijk, Jeffrey E. Saffitz, Frederik A. du Plessis, Michelle Michels, Robert M.W. Hofstra, Richard J. Sinke, J. Peter van Tintelen, Marja W. Wessels, Jan D.H. Jongbloed[^], Ingrid M.B.H. van de Laar[^]

*These authors contributed equally

[^]These authors contributed equally

Journal of the American College of Cardiology 2016;67(5):515-25



Abstract

Background Cardiomyopathies are usually inherited and predominantly affect adults, but they can also present in childhood. Although our understanding of the molecular basis of paediatric cardiomyopathy has improved, the underlying mechanism remains elusive in a substantial proportion of cases.

Objectives This study aimed to identify new genes involved in paediatric cardiomyopathy.

Methods The authors performed homozygosity mapping and whole-exome sequencing in two consanguineous families with idiopathic paediatric cardiomyopathy. Sixty unrelated patients with paediatric cardiomyopathy were subsequently screened for mutations in a candidate gene. First-degree relatives were submitted to cardiac screening and cascade genetic testing. Myocardial samples from two patients were processed for histological and immunohistochemical studies.

Results We identified five patients from three unrelated families with paediatric cardiomyopathy caused by homozygous truncating mutations in *ALPK3*, a gene encoding a nuclear kinase that plays an essential role in early differentiation of cardiomyocytes. All patients with biallelic mutations presented with severe hypertrophic and/or dilated cardiomyopathy in utero, at birth or in early childhood. Three patients died from heart failure within the first week of life. Moreover, two of ten (20%) heterozygous family members showed hypertrophic cardiomyopathy with an atypical distribution of hypertrophy. Deficiency of alpha-kinase 3 has previously been associated with features of both hypertrophic and dilated cardiomyopathy in mice. Consistent with studies in knockout mice, we provide microscopic evidence for intercalated disc remodelling.

Conclusions Biallelic truncating mutations in the newly identified gene *ALPK3* give rise to severe, early-onset cardiomyopathy in humans. Our findings highlight the importance of transcription factor pathways in the molecular mechanisms underlying human cardiomyopathies.

Introduction

Cardiomyopathies represent a clinically and genetically heterogeneous group of disorders affecting the ventricular myocardium. Among children <18 years of age, overall incidence of cardiomyopathy is 1.13 cases per 100,000 annually in the United States.¹ Paediatric cardiomyopathy is associated with significant morbidity and mortality: up to 40% of affected children die or undergo cardiac transplantation within five years of diagnosis.^{2,3} Cardiomyopathy can be classified into five clinical phenotypes based upon morphological and functional characteristics: hypertrophic cardiomyopathy (HCM); dilated cardiomyopathy (DCM); restrictive cardiomyopathy; arrhythmogenic right ventricular (RV) cardiomyopathy; and unclassified cardiomyopathy, including left ventricular (LV) noncompaction.⁴ Extremely diverse, particularly in the paediatric population, the aetiology of cardiomyopathy encompasses both nongenetic and genetic causes, including myocarditis, neuromuscular diseases, inborn errors of metabolism, malformation syndromes, and familial forms caused by mutations in genes encoding the specialized, often structural, components of cardiomyocytes. Because of the routine incorporation of genetic testing in the diagnostic evaluation of patients with cardiomyopathy, a causal diagnosis can be identified in more than 70% of children.⁵ Interestingly, the same genetic causes that result in cardiomyopathy in adults are prevalent in the paediatric population (e.g., sarcomeric or cytoskeletal gene mutations).⁶

Despite recent advances in understanding the genetic aetiologies of paediatric cardiomyopathy, a substantial number of cases remain unsolved, suggesting that other genes await discovery. Establishing an underlying genetic cause for cardiomyopathy allows pre-symptomatic identification of family members at risk and facilitates reproductive decision making. Genetic and genomic studies continue to provide new insights into the pathophysiological processes contributing to cardiomyopathy and will ultimately facilitate development of patient-specific prevention and treatment strategies.

To identify new genes contributing to paediatric cardiomyopathy, we used a combined approach of homozygosity mapping and whole-exome sequencing.

Methods

Patient population

We studied four individuals with paediatric cardiomyopathy from two consanguineous families of Dutch and Moroccan descent, respectively (**Figures 1A** and **1B**). A third family of Turkish descent was identified by subsequent cohort screening (**Figure 1C**). Patients underwent extensive clinical investigations including high-resolution prenatal ultrasound, physical examination, 12-lead electrocardiography, transthoracic echocardiography, and post-mortem examination. Mutation screening of up to 48 known cardiomyopathy-related genes per individual was negative. A complete overview of the genetic and metabolic tests performed before this study is provided in the **Supplemental Information**. All asymptomatic siblings and parents underwent echocardiographic screening. HCM was defined by the presence of increased LV wall thickness (>2 SD above the mean for body surface area in children or ≥ 13 mm in adult relatives) in the absence of hemodynamic stresses sufficient to account for the degree of hypertrophy. DCM was defined by the presence of LV dilatation (LV end-diastolic dimension >2 SD above the mean for body surface area) and systolic dysfunction (fractional shortening or LV ejection fraction >2 SD below the mean for age) in the absence of abnormal loading conditions sufficient to cause global systolic impairment.⁴ A cohort of 60 unrelated patients with idiopathic paediatric cardiomyopathy from diverse ethnic backgrounds was available for mutational screening of candidate genes. These patients had previously been screened for mutations in 8 to 55 known cardiomyopathy-related genes. The medical ethical committees of the University Medical Centre Groningen and the Erasmus University Medical Centre approved this study. Written informed consent was obtained from all participants or their legal guardians.

Homozygosity mapping

Genomic deoxyribonucleic acid (DNA) was extracted from peripheral blood samples (A-VIII:1, VIII:2, IX:1, and IX:2; B-III:1, IV:3, and IV:4), buccal swabs (A-IX:3 and IX:4), amniotic fluid (B-IV:1), or fibroblasts (B-IV:2) (**Figure 1**). Genome-wide genotyping was performed using the Human610-Quad BeadChip (family A) or HumanCytoSNP-12 v2.1 BeadChip (family B) array with raw data normalized and converted into genotypes using GenomeStudio data analysis software (Illumina, San Diego, California). Genotype files were uploaded into the web-based tool HomozygosityMapper to detect homozygous stretches (>5 Mb) in patients that were not present in their unaffected relatives.⁷

Whole exome sequencing

Genomic DNA was sheared by sonication, then the size distribution of fragmented DNA was analysed, targets were captured, and paired-end sequencing (2×101 bp) performed. The sequence reads were mapped and aligned against the human reference genome GRCh37/hg19 (**Supplemental Information**). Variant calling was performed, and variants were filtered

on quality (read depth ≥ 6) and location (within an exon or first/last 20 bp of introns). Variants with a minor allele frequency $\geq 1\%$ in at least 200 chromosomes in dbSNP, the Genome of the Netherlands⁸, the 1000 Genomes Project⁹, or an in-house reference set, or a minor allele frequency $\geq 3\%$ in the National Heart, Lung, and Blood Institute's Go Exome Sequencing Project were excluded from further analysis. Assuming an autosomal recessive model of inheritance, we selected variants found in the heterozygous state in the father and in the homozygous state in the patient. Only variants predicted to change the protein sequence (nonsynonymous single nucleotide variants and short insertions and deletions) or the recognition of consensus ribonucleic acid (RNA) splice sites were considered. Finally, we filtered for variants present in the homozygous regions.

Sanger sequencing

Bidirectional Sanger sequencing of the entire coding region and exon-intron boundaries of the alpha-kinase 3 gene (*ALPK3*) was performed using polymerase chain reaction (PCR) primers (**Supplemental Table 1**). PCR amplification was performed; PCR fragments were purified and sequenced, and then data were analysed (**Supplemental Information**). For annotation of DNA and protein changes, the mutation nomenclature recommendations from the Human Genome Variation Society were followed.¹⁰ Nucleotide numbering reflects complementary DNA (cDNA) numbering with +1 corresponding to the adenine (A) of the ATG translation initiation codon in the reference sequence NM_020778.4.

To assess the effect of the sequence variants identified on protein structure and function, we used prediction programs integrated in the Alamut Visual v2.6.1 software (Interactive Biosoftware, Rouen, France).¹¹⁻¹³ Furthermore, possible effects on splicing were predicted using various integrated algorithm tools.

Reverse transcriptase PCR analysis

To investigate the effect of the splice site variant c.4736-1G>A at the RNA level, we performed reverse-transcription PCR analysis on RNA isolated from fibroblasts of the affected individual (A-IX:2) and two age-matched controls. Cells were cultured in Dulbecco's Modified Eagle Medium supplemented with 10% fetal bovine serum, 1% penicillin/streptomycin, 1% glucose, and 1% glutamax, in atmospheric oxygen and 5% CO₂ at 37°C. Total RNA was extracted, and reverse transcription PCR was performed using gene-specific primers designed to amplify the exon expected to be affected by the mutation and flanking sequences (**Supplemental Figure 1**). The resulting PCR products were examined by 2% agarose gel electrophoresis and subsequently subjected to Sanger sequencing.

Histology

Paraffin-embedded or frozen cardiac tissue was available from two affected individuals (A-IX:2 and B-IV:2). Muscle biopsy specimens from the lateral portion of the quadriceps femoris muscle were available from another affected individual (B-IV:3) and her healthy sister (B-IV:4). Tissues from age-matched donors were used as controls. All samples were histologically examined after haematoxylin and eosin and desmin staining using standard techniques.

Immunohistochemistry

Immunohistochemical analysis was performed on myocardial samples from individual A-IX:2 and two age-matched controls with no clinical or pathological evidence of heart disease, as described previously.¹⁴ In brief, glass-mounted sections of formalin-fixed, paraffin-embedded myocardium (5 µm) were deparaffinised and rehydrated before antibody retrieval. Primary antibodies included mouse monoclonal anti-plakoglobin (1:1,000 dilution), mouse monoclonal anti-plakophilin2 (2a+2b, undiluted), mouse monoclonal anti-desmoplakin (1:10 dilution), mouse monoclonal anti-pan cadherin (1:400 dilution), rabbit polyclonal anti-43 (1:400 dilution), and rabbit polyclonal anti-desmin (1:100 dilution). The slides were then incubated with indocarbocyanine-conjugated goat anti-mouse or goat anti-rabbit secondary antibodies (1:400 dilution). Immunostained preparations were analysed by laser scanning confocal microscopy.

Results

Results are summarized in **Table 1**. In family A, the second child of healthy Dutch parents was born at 35 weeks following an uneventful pregnancy (IX:2) (**Figure 1A**). At birth, he presented with respiratory insufficiency and cyanosis. Echocardiography showed severe LV dilatation (LV end-diastolic dimension 23.5 mm; z-score unreliable because of massive edema) with markedly reduced contractility of both ventricles, and mitral and tricuspid regurgitation. He died due to progressive heart failure at five days. The parents agreed on autopsy (discussed in the Histology section later). Genealogical evaluation revealed that the parents were sixth-degree cousins. Family history was negative for sudden death or cardiomyopathies. Echocardiography revealed no abnormalities in his parents (ages 34 and 31 years), two brothers (ages 9 and 6 years), and sister (age 7 years).

In family B, the first pregnancy of these healthy consanguineous Moroccan parents (IV:1) (**Figure 1B**) included prenatal ultrasound examination at 33 weeks of gestation, revealing generalized hydrops foetalis and cardiomegaly with reduced contractility. The pregnancy ended in intrauterine foetal death at 35 weeks. External examination of the foetus did not show any gross abnormalities except massive skin oedema. Autopsy was declined by the parents. Their second pregnancy resulted in a spontaneous abortion. During the third pregnancy, ultrasound examinations at 20 and 26 weeks of gestation showed an enlarged heart with severely reduced contractility, a thickened myocardium with spongy appearance, and severe tricuspid regurgitation (**Figure 2A**). At 30 weeks of gestation, severe foetal hydrops had developed. The patient was born at 36 weeks (IV:2) (**Figure 1B**) and presented with severe respiratory distress. Echocardiography revealed severe hypertrophy and dilation of both ventricles. She died two hours post-partum. Her parents agreed to a detailed post-mortem examination of the heart (discussed in the Histology section later). In the fourth dizygotic twin pregnancy, extensive prenatal ultrasounds revealed no abnormalities. The twin girls were born at 37 weeks. Echocardiography at day 4 showed severe concentric HCM in one of the twins (IV:3) (**Figure 1B**) which remained stable over subsequent years. Cardiac examination in patient IV:3 at age 10 years showed increased thickness of the interventricular septum (IVS) (IVS thickness 13 mm, z-score +6) and LV posterior wall (LVPW) (LVPW thickness 15 mm, z-score +9.5) (**Figures 2B and 2C**), biventricular diastolic dysfunction, and repolarization abnormalities. There were no ventricular arrhythmias. Family history was negative for sudden cardiac death or cardiomyopathies. Echocardiography revealed no abnormalities in either parent (ages 39 and 22 years) or the twin sister (age 2 months).

Table 1. Clinical features of the affected patients with ALPK3 mutations.

| Individual | Sex | Origin | Age at diagnosis | Presenting symptoms |
|------------|-----|----------|--------------------|---|
| A-IX:2 | M | Dutch | At birth | Severe biventricular dilation |
| B-IV:1 | F | Moroccan | 33 weeks gestation | Generalized hydrops foetalis, cardiomegaly |
| B-IV:2 | F | Moroccan | 20 weeks gestation | Generalized hydrops foetalis, severe biventricular hypertrophy and dilation, severe tricuspid regurgitation |
| B-IV:3 | F | Moroccan | At birth | Severe concentric LV hypertrophy |
| C-IV:1 | M | Turkish | 29 years | Asymmetrical septum hypertrophy, RV hypertrophy |
| C-IV:2 | M | Turkish | 27 years | Concentric LV hypertrophy with relative sparing of basal segments, RV hypertrophy |
| C-V:2 | M | Turkish | 4 years | Severe concentric LV hypertrophy, RV hypertrophy |

ALPK3=alpha-kinase 3 gene, D=death, F=female, ICD=implantable cardioverter-defibrillator, LV=left ventricular, M=male, RV=right ventricular

For family C, the index patient (C-V:2) was the second child of consanguineous Turkish parents. He was diagnosed with severe HCM at 4 years of age with subsequent slow disease progression. Out-of-hospital cardiac arrest occurred at age 7 years due to ventricular arrhythmias, after which an implantable cardiac-defibrillator (ICD) was placed; he has since experienced several appropriate ICD shocks. Cardiac examination at age 11 years showed severe concentric LV hypertrophy (IVS 20 mm, z-score +11.2; LVPW 19 mm, z-score +13.1) without LV outflow tract obstruction (**Figures 2D** and **2E**), moderate hypertrophy of the right ventricle (RV), and repolarization abnormalities. His father (C-IV:2) was diagnosed with HCM at age 27 years. Cardiac magnetic resonance imaging at age 37 years showed concentric LV hypertrophy, most pronounced in the septum (IVS 32 mm) with relative sparing of the basal segments, and RV hypertrophy (**Figure 2F**). Echocardiographic screening in the mother (age 42 years) and older brother (age 19 years) revealed no abnormalities. A paternal uncle (C-IV:1) had been diagnosed with HCM at 29 years. Cardiac examination at 45 years of age showed asymmetric septal hypertrophy (IVS 17 mm; LVPW 11 mm) and RV hypertrophy (7 to 8 mm; normal cutoff: 5 mm).

Homozygosity mapping

In family A, we identified two chromosomal regions that were homozygous in the affected boy (IX:2) and heterozygous in his parents (VIII:1 and VIII:2) and unaffected brother (IX:1): 15q25.2q25.3 (84,058,592 to 89,164,874) and 21q21.3q22.11 (29,440,969 to 35,838,907). In family B, we identified three homozygous chromosomal regions shared by all affected individuals

| Outcome | Genotype |
|---|---|
| D. 5 days postpartum | Homozygous c.4736-1G>A, p.(Val1579Glyfs*30) |
| D. 36 weeks gestation | Homozygous c.3781C>T, p.(Arg1261*) |
| D. 2 hours postpartum | Homozygous c.3781C>T, p.(Arg1261*) |
| Status quo (11 years) | Homozygous c.3781C>T, p.(Arg1261*) |
| Status quo (45 years) | Heterozygous c.5294G>A, p.(Trp1765*) |
| Status quo (43 years) | Heterozygous c.5294G>A, p.(Trp1765*) |
| Ventricular fibrillation, ICD implantation (7 years) | Homozygous c.5294G>A, p.(Trp1765*) |

(IV:1, IV:2 and IV:3), whereas the unaffected father (III:1) and sister (IV:4) were heterozygous: 5q14.3q15 (90,263,863 to 95,782,290), 15q25.1q25.3 (79,333,228 to 87,165,178) and 16q23.2q24.3 (81,602,681 to 90,148,796) (NCBI Build GRCh37/hg19). A small region (3.1 Mb) of homozygosity on chromosome region 15q25 overlapped between the affected individuals from both families.

Exome variant filtering

Exome sequencing was performed to target all exons and exon-intron junction sequences of known genes in the human genome for potential disease-causing variants. Using the filtering pipeline discussed earlier, affected individuals from families A and B were found to harbour a homozygous variant in the *ALPK3* gene (**Supplemental Table 2**), located in the overlapping region of homozygosity on chromosome 15q25. Patient A-IX:2 was found to carry a homozygous intronic variant in the consensus acceptor splice site sequence of exon 10 of the *ALPK3* gene (c.4736-1G>A) (**Figure 3**), and this result was validated using Sanger sequencing. Both parents and two unaffected siblings (A-IX:1 and IX:3) were heterozygous for the mutation. One unaffected sibling (A-IX:4) carried the normal genotype. Patient B-IV:3 harboured a homozygous variant in exon 6 of the *ALPK3* gene introducing a premature stop codon (c.3781C>T, p.(Arg1261*)) (**Figure 3**). Sanger sequencing proved that all affected children were homozygous for this mutation. The father and unaffected sibling (B-IV:4) were heterozygous for the mutation. The mother was unavailable for testing, but is presumed to be a heterozygous carrier of the mutation as well.

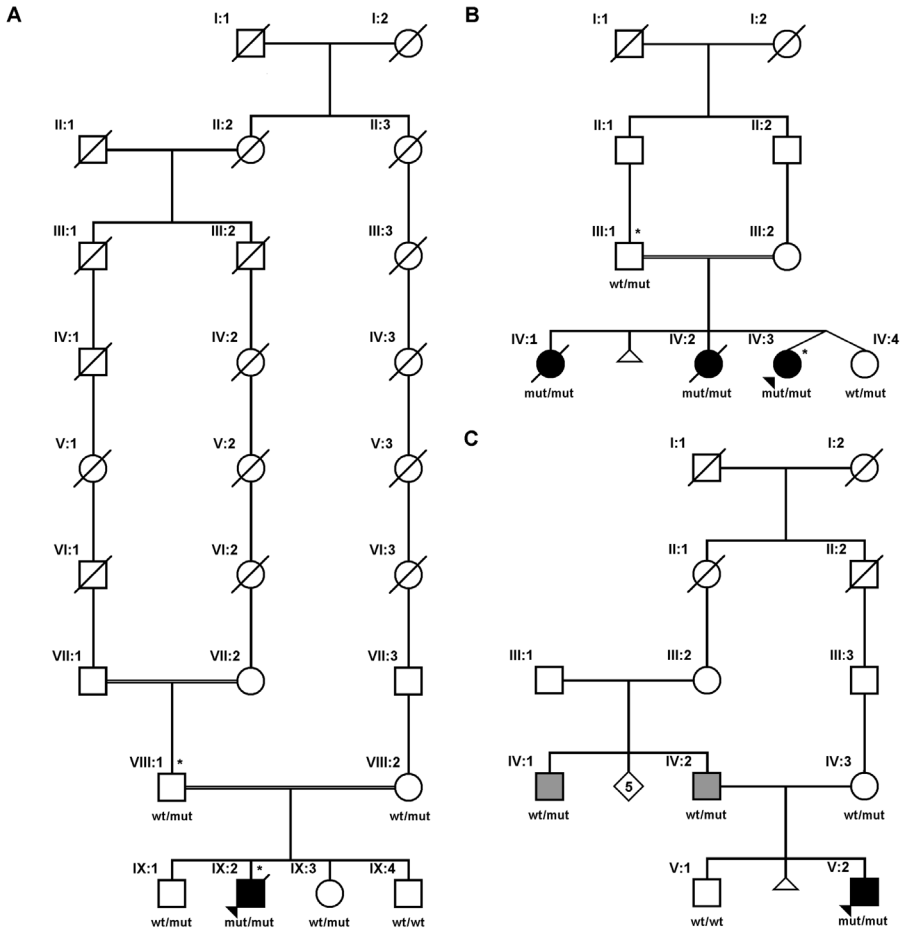


Figure 1. ALPK3-related cardiomyopathy. Pedigrees of families (A, B, and C) with alpha-kinase 3 (ALPK3) genetic mutation leading to cardiomyopathy. Asterisks = analysed by exome sequencing, squares = males, circles = females, solid symbols = severely affected individuals with homozygous mutations, gray symbols = heterozygous individuals with adult-onset disease, open symbols = unaffected individuals, diagonal lines = deceased, arrowheads = index patients. ALPK3 genotypes: mut = mutant allele, wt = wild-type allele.

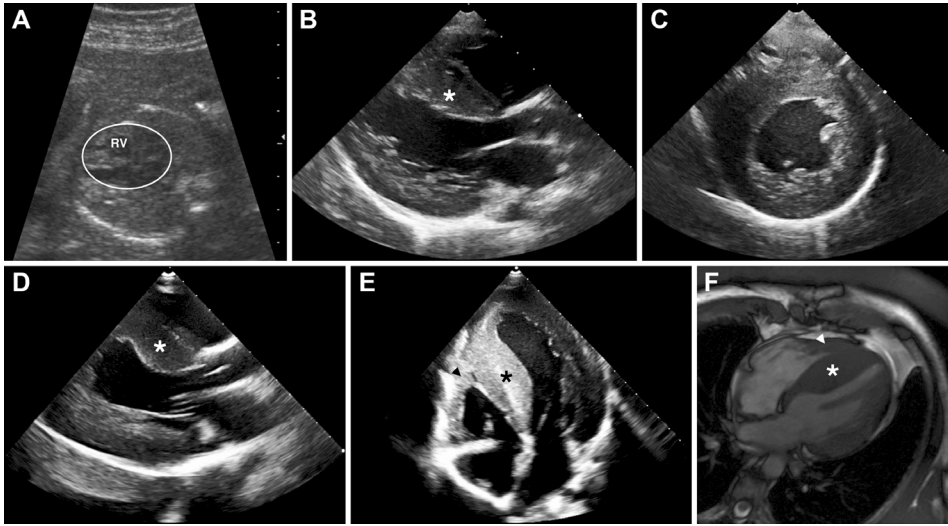


Figure 2. Cardiac imaging in ALPK3-related cardiomyopathy. Prenatal ultrasound performed in patient B-IV:2 at 20 weeks of gestation showed an enlarged heart (encircled) with right ventricular (RV) hypertrophy. (A) Echocardiographic images of the parasternal long-axis (B) and short-axis (C) views in patient B-IV:2 showed severe concentric left ventricular (LV) hypertrophy. Parasternal long-axis (D) and 4-chamber (E) views in patient C-V:2 showed severe concentric LV hypertrophy and moderate RV hypertrophy. (F) Cardiac magnetic resonance image in patient C-IV:2 showed atypical distribution of LV hypertrophy with relative sparing of the basal segments, and RV hypertrophy. Asterisks = interventricular septum, arrowhead = RV hypertrophy. Abbreviations as in **Figure 1**.

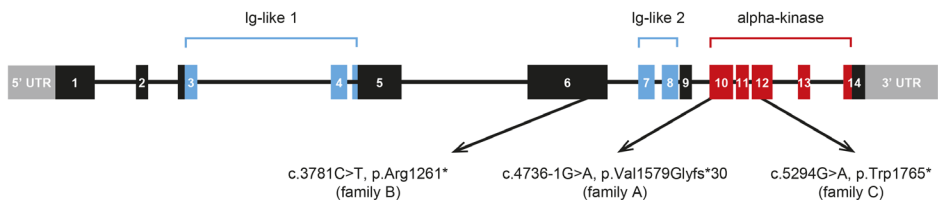


Figure 3. ALPK3 gene schematic. The 3 main functional domains - 2 immunoglobulin (Ig)-like domains (blue) and 1 alpha-type protein kinase domain (red) - and the positions of identified ALPK3 mutations are indicated. Boxes = exons and untranslated regions (UTR), connecting lines = intervening introns. Abbreviations as in **Figure 1**.

ALPK3 mutational screening

Subsequent Sanger sequencing of all coding regions and flanking intronic sequences of the *ALPK3* gene in a cohort of 60 unrelated patients with childhood-onset HCM or DCM uncovered the homozygous nucleotide substitution c.5294G>A in exon 12 introducing a premature stop codon (p.(Trp1765*)) in a third patient (family C) (**Figure 1C, Table 1**). His affected father and paternal uncle were heterozygous carriers; no additional mutation in the known cardiomyopathy genes was found (**Supplemental Information**). In the remaining cohort, no additional mutations in *ALPK3* were identified. Further studies will be performed in these patients to discover novel disease genes.

Splice variant analysis

The c.4736-1G>A variant in intron 9 (family A) was predicted to impair the natural acceptor splice site recognition using *in silico* tools. Sanger sequencing of cDNA from cultured fibroblasts of patient A-IX:2 confirmed skipping of exon 10, leading to a deletion of 281 nucleotides (**Supplemental Figure 1**). At the protein level, a frameshift starting at codon Val1579 and ending in a stop codon 29 positions downstream (p.(Val1579Glyfs*30)) is predicted.

Histology

Post-mortem macroscopic examination of the heart of individual A-IX:2 revealed severe cardiomegaly (total weight 34.0 g; normal 13.7 g) and biventricular dilation. Microscopic examination of the myocardium showed subendocardial fibroelastosis without fatty replacement in both ventricles, fragmented elastin fibers, and myxoid degeneration of the stroma (**Figure 4A**). Post-mortem macroscopic examination of the heart of individual B-IV:2 revealed severe cardiomegaly (total weight 34.7 g; normal 15.5 g) and biventricular dilation with a large adherent thrombus to the left ventricle. Microscopic examination showed focal hypertrophy of the cardiomyocytes and extensive fibroelastosis in the subendocardial region without fatty infiltration (**Figures 4B and 4C**). No apparent myocyte disarray was observed both on evaluation with haematoxylin and eosin staining, and immunohistochemical staining for desmin (**Figure 4D**). Intercalated discs were difficult to recognize in both the patients and age-matched controls. Muscle biopsies from individual B-IV:3 (affected) and B-IV:4 (unaffected carrier) did not show any changes at routine histological and enzyme histochemical evaluation, including acid phosphatase, nicotinamide adenine dinucleotide + hydrogen-tetrazolium reductase, succinate dehydrogenase, and cytochrome C oxidase.

Immunohistochemistry

To determine the effects of *ALPK3* mutations at the level of the intercalated discs, we performed immunohistochemical analysis of junctional proteins in cardiac tissue from one patient (A-IX:2) and two age-matched controls. Immunoreactive signal levels for the desmosomal proteins plakoglobin and desmoplakin were absent at intercalated discs in the patient sample. Signal levels for the other desmosomal protein plakophilin-2, the adhesion molecule N-cadherin, and the gap-junction protein connexin-43 were normal compared with controls (**Figure 5**). Results of desmin staining were inconclusive (data not shown), as intercalated discs were difficult to recognize in both the patient and control samples.

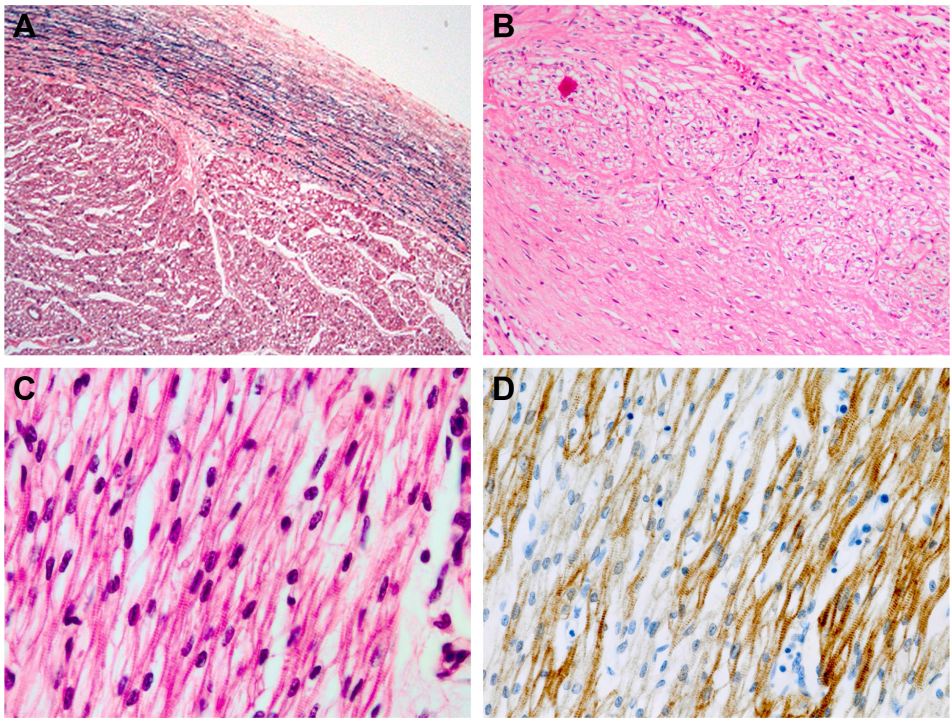


Figure 4. Histopathological examination of heart tissue in *ALPK3*-related cardiomyopathy. In patient A-IX:2, Verhoeff-van Gieson staining for elastin at 20 x magnification showed subendocardial fibroelastosis (A). In patient B-IV:2, hematoxylin and eosin staining at 100 x (B) and 630 x magnification (C) showed focal hypertrophy of cardiomyocytes and subendocardial fibroelastosis without fatty infiltration; desmin staining (D) showed no apparent myocyte disarray. Intercalated discs were difficult to recognize in patient B-IV:2 and age-matched controls (data not shown). Abbreviations as in **Figure 1**.

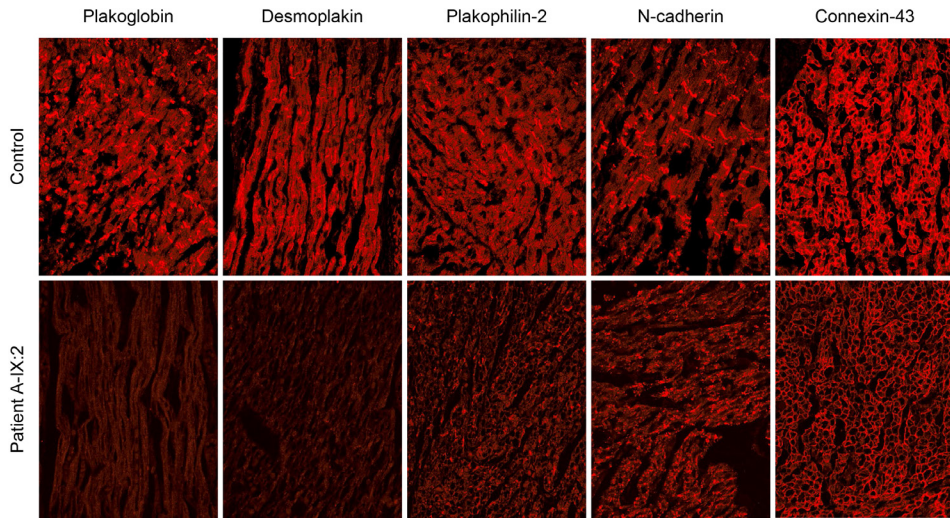


Figure 5. Immunofluorescence images of myocardial tissue. Immunoreactive signals for plakoglobin and desmoplakin are absent at intercalated discs in the sample from patient A-IX:2, whereas signal levels for plakophilin-2, N-cadherin and connexin-43 are normal when compared with the control samples.

Discussion

We identified a novel gene, *ALPK3*, involved in human cardiomyopathy (**Central Illustration**). Biallelic truncating *ALPK3* mutations were identified in five patients with diverse ethnic backgrounds who presented with severe, early-onset cardiomyopathy. Four patients were diagnosed during foetal life or within hours of birth. The fifth patient was asymptomatic until the age of 4 years. Three out of five patients died due to progressive heart failure between 35 weeks of gestation and five days after birth. The patients who died exhibited features of DCM or a combination of DCM and HCM. Two patients, who were still alive at age 11 years, showed severe concentric HCM. Although classic HCM and DCM primarily affect the left ventricle, three patients also displayed significant RV involvement. Interestingly, two heterozygous family members (C-IV:1 and IV:2) were diagnosed with an atypical form of HCM at a young adult age. Cardiac examination of the other proven and obligate heterozygotes ($n = 8$; age range: 2 months to 42 years) revealed no evidence of cardiomyopathy. Although these numbers are limited, one may surmise that *ALPK3* mutation carriers have an increased risk of developing cardiomyopathy; therefore, periodic screening should be considered.

The *ALPK3* gene is the human ortholog of the murine Myocytic induction/differentiation originator (also known as *Midori*). In 2001, the *Alpk3* gene was identified by applying a differential display technique in the P19CL6 cell line, which can be differentiated into beating cardiomyocytes upon incubation with dimethyl sulfoxide. Overexpression of *Alpk3* promoted their differentiation into cardiomyocytes, whereas differentiation was inhibited by blockade of *Alpk3* expression.¹⁵ The gene has been mapped to chromosome 15q25.2 and contains 14 exons (**Figure 3**). The *ALPK3* protein contains two immunoglobulin (Ig)-like domains and an alpha-type protein kinase domain. All three private homozygous mutations identified in this study are predicted to create premature stop codons, leading to nonsense-mediated decay or truncated proteins with partial or complete removal of the kinase domain (**Figure 3**). We therefore hypothesize that these mutations result in loss of function of *ALPK3*. Alpha-kinase 3 belongs to a family of atypical protein kinases that recognize phosphorylation sites in the context of alpha-helices. Alpha-kinases are known to regulate a wide range of cellular processes, including cell migration, adhesion and proliferation, protein translation, vesicular transport and magnesium homeostasis.^{16,17}

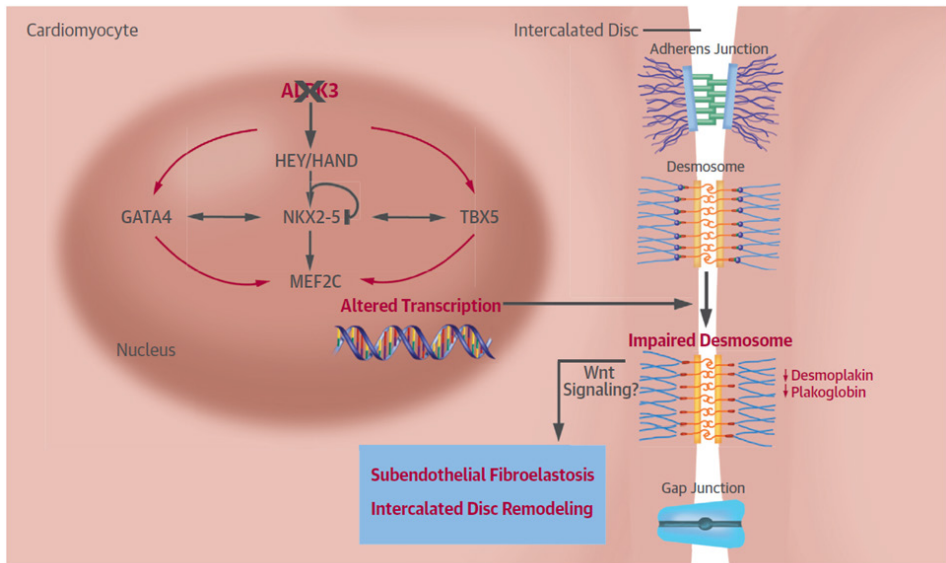
In mouse embryos, expression of *Alpk3* was restricted to foetal and adult hearts and adult skeletal muscle. Interestingly, *Alpk3* knockout mice display cardiomyopathy with striking similarities to the human phenotype described here.¹⁸ Although concentric cardiac hypertrophy of both the left and right ventricle was the predominant feature in *Alpk3*-deficient mice, other changes typically associated with DCM were also observed such as increased end-diastolic and end-systolic LV volume and a reduction in cardiac outflow, stroke volume, and ejection fraction.¹⁸

Detailed histological and ultrastructural analysis of hearts from *Alpk3*^{-/-} mice showed markedly reduced numbers of indistinct and fragmented intercalated discs and diffuse mild myofibrillar disarray, resulting in looser arrangement of adjacent myofibrils.¹⁸ Interstitial fibrosis, one of the pathological hallmarks of cardiomyopathies, was absent. In contrast to the observations in *Alpk3* knockout mice, we observed extensive fibroelastosis without apparent myocyte disarray in our human cardiac samples (**Figure 4**).

Intercalated discs play an essential role in the mechanical and electrochemical coupling between adjacent cardiomyocytes. There are three main junctional complexes within the disc: fascia adherens, desmosomes, and gap junctions. At an early age, intercalated discs are difficult to visualize under light microscopy, as exemplified in this study. Unfortunately, no patient material was available for ultrastructural examination using electron microscopy. However, immunohistochemical analysis in myocardial tissue from one patient revealed the absence of desmosomal proteins plakoglobin and desmoplakin signals at the intercalated discs, whereas signals for the other junctional proteins were normal (**Figure 5**). Reduced immunoreactive signals for plakoglobin at cell-cell junctions have been observed in the majority of patients with arrhythmogenic RV cardiomyopathy. The specificity of this finding, however, remains under debate.^{14,19} Redistribution of plakoglobin from intercellular junctions to the intracellular space is believed to suppress canonical Wnt/beta-catenin signalling, leading to enhanced fibrogenesis and myocyte apoptosis.²⁰ Reduced signal levels for desmoplakin at intercalated discs, on the other hand, have mainly been demonstrated in patients with end-stage DCM due to mutations in the gene encoding desmin.²¹ Although our findings support a role for *ALPK3* in the formation and maintenance of intercalated discs, further studies in a larger cohort of patients are needed for validation.

The molecular mechanisms involved in the earliest stages of cardiac development are still largely unknown. *ALPK3* is expressed from the very early stage of cardiogenesis, before key transcription factors, such as the NK-2 class homeobox transcription factor *NKX2-5*, the GATA-binding protein *GATA4*, and the MADS-box transcription enhancer factor *MEF2C*.¹⁵ Some cardiac transcription factors (e.g., HEY and HAND proteins) contain a helix-loop-helix domain, characterized by two alpha helices separated by a flexible loop structure, and might therefore be targets of *ALPK3*. By regulating the expression of these transcription factors, *ALPK3* might control initial induction of differentiation and maturation of cardiomyocytes. Mutations in these putative downstream targets of *ALPK3* have previously been associated with various congenital heart malformations and arrhythmias in humans.²² Structural heart abnormalities were not observed in the patients described in this study. In recent years, however, some of these genes have also been implicated in familial forms of cardiomyopathy, including *NKX2-5*, *GATA4*, *GATA6*, and the T-box transcription factors *TBX5* and *TBX20*.²³⁻²⁷ Interestingly, mice lacking Xin actin-binding repeat-containing protein 1 (*Xirp1*), a downstream target of *Nkx2-5* and *Mef2c*, display intercalated discs abnormalities and cardiac hypertrophy with conduction defects.²⁸ Further

research into the transcription factor pathways involved in heart development and the putative role of ALPK3 in the related processes will provide more insight into the molecular pathways involved in paediatric cardiomyopathy and may have implications for the development of new therapeutic strategies.



Central Illustration. ALPK3-related cardiomyopathy: hypothetical disease model. Deficiency of alpha-kinase 3 (ALPK3) modifies the expression of other transcription factors and downstream target genes. These changes affect desmosome composition and will, putatively via modified Wnt signalling, ultimately result in alterations of cellular processes, like subendothelial fibroelastosis and intercalated disc remodelling, characteristic of cardiomyopathy.

Study limitations

Although our finding that ALPK3 is the causal gene in three unrelated families of different ethnic backgrounds with paediatric cardiomyopathy underscores its contribution to this severe disease, studies in other and larger cohorts to substantiate our findings are warranted. Further protein studies and electron microscopy examination are needed to fully understand the effects of ALPK3 mutations and to enhance our understanding of underlying mechanisms leading to the clinical phenotype. For example, immunolabeling with ALPK3 antibodies would give insight into its expression in cardiac tissue. Moreover, identifying interacting partner proteins of ALPK3 will lead to identifying downstream-acting proteins involved in the pathogenesis and remodelling of intercalated discs. Unfortunately, these studies are hampered by the limited availability of cardiac tissues of the patients.

Conclusions

We have shown that biallelic truncating mutations in *ALPK3* lead to severe, early-onset paediatric cardiomyopathy in humans. Carriers may develop cardiomyopathy as adults. *ALPK3*-related cardiomyopathy has morphological features of both HCM and DCM, and is characterized by biventricular involvement and atypical distribution of hypertrophy. Our findings emphasize the essential role of cardiac transcription factor pathways in normal myocardial development. Further studies are necessary to understand how dysregulation of the transcriptional regulatory network results in cardiomyopathy (**Central Illustration**).

Acknowledgements

The authors thank the families for participating in this study. The authors would like also to thank Kate McIntyre for editing this manuscript, and Tom de Vries Lentsch and René Frowijn for photographic artwork.

Conflict of Interest

The authors declare no conflict of interest.

Funding

This work was supported by funding from the Dutch Heart Foundation (2007B132, 2010B164 and 2014T007).

References

1. Lipshultz SE, Sleeper LA, Towbin JA, et al. The incidence of pediatric cardiomyopathy in two regions of the United States. *N Engl J Med* 2003;348:1647-1655.
2. Daubeny PE, Nugent AW, Chondros P, et al. Clinical features and outcomes of childhood dilated cardiomyopathy: results from a national population-based study. *Circulation* 2006;114:2671-2678.
3. Towbin JA, Lowe AM, Colan SD, et al. Incidence, causes, and outcomes of dilated cardiomyopathy in children. *JAMA* 2006;296:1867-1876.
4. Elliott P, Andersson B, Arbustini E, et al. Classification of the cardiomyopathies: a position statement from the European Society Of Cardiology Working Group on Myocardial and Pericardial Diseases. *Eur Heart J* 2008;29:270-276.
5. Kindel SJ, Miller EM, Gupta R, et al. Pediatric cardiomyopathy: importance of genetic and metabolic evaluation. *J Card Fail* 2012;18:396-403.
6. Tariq M, Ware SM. Importance of genetic evaluation and testing in pediatric cardiomyopathy. *World J Cardiol* 2014;6:1156-1165.
7. Seelow D, Schuelke M. HomozygosityMapper2012--bridging the gap between homozygosity mapping and deep sequencing. *Nucleic Acids Res* 2012;40:W516-20.
8. Boomsma DI, Wijmenga C, Slagboom EP, et al. The Genome of the Netherlands: design, and project goals. *Eur J Hum Genet* 2014;22:221-227.
9. 1000 Genomes Project Consortium, Abecasis GR, Auton A, et al. An integrated map of genetic variation from 1,092 human genomes. *Nature* 2012;491:56-65.
10. den Dunnen JT, Antonarakis SE. Mutation nomenclature extensions and suggestions to describe complex mutations: a discussion. *Hum Mutat* 2000;15:7-12.
11. Ng PC, Henikoff S. Predicting deleterious amino acid substitutions. *Genome Res* 2001;11:863-874.
12. Adzhubei IA, Schmidt S, Peshkin L, et al. A method and server for predicting damaging missense mutations. *Nat Methods* 2010;7:248-249.
13. Schwarz JM, Cooper DN, Schuelke M, Seelow D. MutationTaster2: mutation prediction for the deep-sequencing age. *Nat Methods* 2014;11:361-362.
14. Asimaki A, Tandri H, Huang H, et al. A new diagnostic test for arrhythmogenic right ventricular cardiomyopathy. *N Engl J Med* 2009;360:1075-1084.
15. Hosoda T, Monzen K, Hiroi Y, et al. A novel myocyte-specific gene Midori promotes the differentiation of P19CL6 cells into cardiomyocytes. *J Biol Chem* 2001;276:35978-35989.
16. Middelbeek J, Clark K, Venselaar H, Huynen MA, van Leeuwen FN. The alpha-kinase family: an exceptional branch on the protein kinase tree. *Cell Mol Life Sci* 2010;67:875-890.
17. Drennan D, Ryazanov AG. Alpha-kinases: analysis of the family and comparison with conventional protein kinases. *Prog Biophys Mol Biol* 2004;85:1-32.
18. Van Sligtenhorst I, Ding ZM, Shi ZZ, Read RW, Hansen G, Vogel P. Cardiomyopathy in alpha-kinase 3 (ALPK3)-deficient mice. *Vet Pathol* 2012;49:131-141.
19. Munkholm J, Christensen AH, Svendsen JH, Andersen CB. Usefulness of immunostaining for plakoglobin as a diagnostic marker of arrhythmogenic right ventricular cardiomyopathy. *Am J Cardiol* 2012;109:272-275.

20. Garcia-Gras E, Lombardi R, Giocondo MJ, et al. Suppression of canonical Wnt/beta-catenin signaling by nuclear plakoglobin recapitulates phenotype of arrhythmogenic right ventricular cardiomyopathy. *J Clin Invest* 2006;116:2012-2021.
21. Otten E, Asimaki A, Maass A, et al. Desmin mutations as a cause of right ventricular heart failure affect the intercalated disks. *Heart Rhythm* 2010;7:1058-1064.
22. McCulley DJ, Black BL. Transcription factor pathways and congenital heart disease. *Curr Top Dev Biol* 2012;100:253-277.
23. Pashmforoush M, Lu JT, Chen H, et al. Nkx2-5 pathways and congenital heart disease; loss of ventricular myocyte lineage specification leads to progressive cardiomyopathy and complete heart block. *Cell* 2004;117:373-386.
24. Li RG, Li L, Qiu XB, et al. GATA4 loss-of-function mutation underlies familial dilated cardiomyopathy. *Biochem Biophys Res Commun* 2013;439:591-596.
25. Xu L, Zhao L, Yuan F, et al. GATA6 loss-of-function mutations contribute to familial dilated cardiomyopathy. *Int J Mol Med* 2014;34:1315-1322.
26. Zhang XL, Qiu XB, Yuan F, et al. TBX5 loss-of-function mutation contributes to familial dilated cardiomyopathy. *Biochem Biophys Res Commun* 2015;459:166-171.
27. Kirk EP, Sunde M, Costa MW, et al. Mutations in cardiac T-box factor gene TBX20 are associated with diverse cardiac pathologies, including defects of septation and valvulogenesis and cardiomyopathy. *Am J Hum Genet* 2007;81:280-291.
28. Gustafson-Wagner EA, Sinn HW, Chen YL, et al. Loss of mXinalpha, an intercalated disk protein, results in cardiac hypertrophy and cardiomyopathy with conduction defects. *Am J Physiol Heart Circ Physiol* 2007;293:H2680-92.

Supplemental Information

Detailed methods

Overview of previous genetic and metabolic testing

Patient A-IX:2. Biochemical studies, including analysis of blood glucose, lactate, pyruvate, creatine kinase, amino acids, acylcarnitines, and sialotransferrin levels were normal. Total and free carnitine levels were extremely elevated due to supplementation and massive cellular tissue death. Enzyme studies in fibroblasts showed normal carnitine palmitoyltransferase I and II, α and β -glucosidase, and β -galactosidase activities. Monolysocardiolipin/cardioliipin ratio was normal. Viral serology showed no abnormalities. Sanger sequencing of the genes *DES* (NM_001927.3), *LMNA* (NM_001257374.2), *MYBPC3* (NM_000256.3), *MYH7* (NM_000257.3), *MYL2* (exon 7, NM_000432.3), *TAZ* (NM_181312.3), *TNNI3* (NM_000363.4) and *TNNT2* (NM_001001430.2) revealed no abnormalities.

Patient B-IV:1. Conventional karyotyping results of amniotic fluid cells were normal (46,XX). Serological testing for intrauterine infections showed elevated IgM antibodies for herpes simplex virus (HSV). Post-mortem nasal and throat swabs were negative for HSV.

Patient B-IV:2. Conventional karyotyping results were normal (46,XX). Microbiological studies, including PCR, serology and blood and ascites cultures, were negative. Extensive metabolic screening, including analysis of blood glucose, lactate, amino acids, organic acids, total and free carnitine, acylcarnitines and very long-chain fatty acids levels revealed no evidence of an inborn error of metabolism. Isoelectric focusing of serum transferrin was normal. Enzyme studies in fibroblasts showed normal hexosaminidase A and B, β -galactosidase, α and β -glucosidase, β -glucuronidase, galactose-6-sulfatase, galactosyl ceramidase, iduronate 2-sulfatase, α -iduronidase, sphingomyelinase, neuraminidase and phosphomannomutase activities. Mutation analysis of common mitochondrial DNA point mutations (A3243G, A8344G, T8933G/C, A3260G, A4300G, A4269G and A4317G) and deletions revealed no abnormalities.

Patient B-IV:3. Extensive metabolic screening, including analysis of blood glucose, lactate, pyruvate, amino acids, organic acids, total and free carnitine, acylcarnitines, oligosaccharides, sialic acids, and very long-chain fatty acids levels revealed no evidence of an inborn error of metabolism. Isoelectric focusing of serum transferrin was normal. Enzyme activity studies of the individual complexes of the respiratory chain showed no abnormalities. Next-generation sequencing (paired-end 150 bp, Miseq, Illumina) of 46 cardiomyopathy-related genes showed a homozygous variant, c.393-5C>A, in the *SCN5A* gene (NM_000335.4). This variant has been reported in heterozygous state in a patient with long QT syndrome and has been found at a low frequency in several populations (rs368678204).¹ However, this variant was also

present in 3 out of 93 Moroccan control samples. In addition, RT-PCR analysis showed that this variant does not affect splicing (data not shown). The variant was therefore classified as “likely benign” (class 2). Analysis of the other 45 genes, *ABCC9* (NM_020297.2), *ACTC1* (NM_005159.4), *ACTN2* (NM_001103.2), *ANKRD1* (NM_014391.2), *BAG3* (NM_004281.3), *CALR3* (NM_145046.3), *CASQ2* (NM_001232.2), *CAV3* (NM_033337.2), *CRYAB* (NM_001885.1), *CSRP3* (NM_003476.3), *DES* (NM_001927.3), *EMD* (NM_000117.2), *FHL1* (NM_001159702.2), *FKTN* (NM_001079802.1), *GLA* (NM_000169.2), *ILK* (NM_004517.2), *JPH2* (NM_020433.4), *LAMA4* (NM_001105206.1), *LAMP2* (NM_002294.2), *LDB3* (NM_007078.2), *LMNA* (NM_170707.2), *MYBPC3* (NM_000256.3), *MYH7* (NM_000257.2), *MYL2* (NM_000432.3), *MYL3* (NM_000258.2), *MYOZ2* (NM_016599.3), *MYPN* (NM_032578.2), *NEXN* (NM_144573.3), *NRG1* (NM_013956.3), *PDLIM3* (NM_014476.4), *PLN* (NM_002667.3), *PRKAG2* (NM_016203.3), *RBM20* (NM_001134363.1), *SGCD* (NM_000337.5), *TAZ* (NM_000116.3), *TBX20* (NM_001077653.2), *TCAP* (NM_003673.3), *TMPO* (NM_003276.2), *TNNC1* (NM_003280.2), *TNNI3* (NM_000363.4), *TNNT2* (NM_001001430), *TPM1* (NM_001018005.1), *TTN* (NM_003319.4), *TTR* (NM_000371.3) and *VCL* (NM_014000.2) revealed no abnormalities.

Patient C-IV:2. Sanger sequencing of the genes *ACTC1* (NM_005159), *CSRP3* (NM_003476.2), *MYBPC3* (NM_000256), *MYH7* (NM_000257), *MYL2* (NM_000432), *TCAP* (NM_003673.2), *TNNI3* (NM_000363), *TNNT2* (NM_001001430.1) and *TPM1* (NM_000366; NM_001018005) revealed no abnormalities. Next-generation sequencing (paired-end 150 bp, Miseq, Illumina) of 48 cardiomyopathy-related genes showed two heterozygous missense variants, c.61922G>A, p.(Arg20641Gln) and c.98294C>G, p.(Ala32765Gly), in the *TTN* gene (NM_001267550.1). These variants have been found at a low frequency in various populations (rs199895260 and rs72648273, respectively) and were classified as “variant of unknown significance” (class 3). Analysis of the other 47 genes, *ABCC9* (NM_020297.2; NM_020298.2), *ACTC1* (NM_005159.4), *ACTN2* (NM_001103.2), *ANKRD1* (NM_014391.2), *BAG3* (NM_004281.3), *CALR3* (NM_145046.3), *CAV3* (NM_033337.3), *CRYAB* (NM_001885.1), *CSRP3* (NM_003476.3), *CTNNA3* (NM_013266.2), *DES* (NM_001927.3), *DSC2* (NM_024422.3; NM_004949.3), *DSG2* (NM_001943.3), *DSP* (NM_004415.2), *EMD* (NM_000117.2), *FHL1* (NM_001159699.1; NM_001159701.1; NM_001159702.2;), *GLA* (NM_000169.2), *JPH2* (NM_020433.4; NM_175913.3), *JUP* (NM_021991.2), *LAMA4* (NM_001105206.1; NM_001105208.1), *LAMP2* (NM_001122606.1; NM_002294.2; NM_013995.2), *LDB3* (NM_001080116.1; NM_007078.2), *LMNA* (NM_001257374.1; NM_005572.3; NM_170707.3), *MIB1* (NM_020774.2), *MYBPC3* (NM_000256.3), *MYH6* (NM_002471.3), *MYH7* (NM_000257.2), *MYL2* (NM_000432.3), *MYL3* (NM_000258.2), *MYOZ2* (NM_016599.3), *MYPN* (NM_032578.2), *NEXN* (NM_144573.3), *PKP2* (NM_004572.3), *PLN* (NM_002667.3), *PRDM16* (NM_22114.3), *PRKAG2* (NM_016203.3), *RBM20* (NM_001134363.1), *SCN5A* (NM_001160160.1; NM_198056.2), *TAZ* (NM_000116.3), *TCAP*

(NM_003673.3), *TMEM43* (NM_024334.2), *TNNC1* (NM_003280.2), *TNNI3* (NM_000363.4), *TNNT2* (NM_000364.2; NM_001001430.1), *TPM1* (NM000366.5; NM_001018005.1; NM_001018020.1), *TTR* (NM_000371.3) and *VCL* (NM_014000.2) revealed no abnormalities. SNP array analysis (Infinium CytoSNP-850K BeadChip) showed a normal male pattern.

Patient C-V:2. Metabolic screening, including analysis of amino acids, organic acids, sialic acids, total and free carnitine, acylcarnitines, oligosaccharides and mucopolysaccharides levels revealed no evidence of an inborn error of metabolism. SNP array analysis (Affymetrix GeneChip Human Mapping 250K Nsp) showed several large regions of homozygosity, consistent with known parental consanguinity.

Whole exome sequencing

Genomic DNA was sheared by sonication (Covaris, Woburn, MA, USA). Size distribution of fragmented DNA was analysed on an Agilent 2100 Bioanalyzer System using the DNA 1000 kit. Targets were captured with the SureSelect Human All Exon 50 Mb kit V4 (Agilent Technologies, Santa Clara, CA, USA). Paired-end sequencing (2x101 bp) was performed on an Illumina HiSeq2000 platform (Illumina, San Diego, CA, USA). The sequence reads were mapped and aligned against the human reference genome GRCh37/hg19 with the Burrows-Wheeler Aligner.² Variant calling was performed using the Genome Analysis Toolkit (GATK) and SAMtools.^{3,4} Variant filtering was performed using Cartagenia Bench Lab NGS version 4.02 (Cartagenia, Leuven, Belgium).

Sanger sequencing

Polymerase chain reaction (PCR) was performed prior to Sanger sequencing. PCR primers were designed by Primer3 software (<http://bioinfo.ut.ee/primer3/>). PCR amplification was performed using the AmpliTaq Gold 360 Master Mix (Invitrogen, Life Technologies, Carlsbad, CA, USA) following the manufacturer's protocol. PCR fragments were purified with ExoSAP-IT (Affymetrix, Santa Clara, CA, USA) and subsequently sequenced on an ABI3730xl DNA Analyzer using BigDye Terminator v3.1 (Applied Biosystems, Foster City, CA, USA). Analysis of sequence data was performed using Mutation Surveyor (SoftGenetics, State College, PA, USA) and SeqScape v2.5 software (Applied Biosystems).

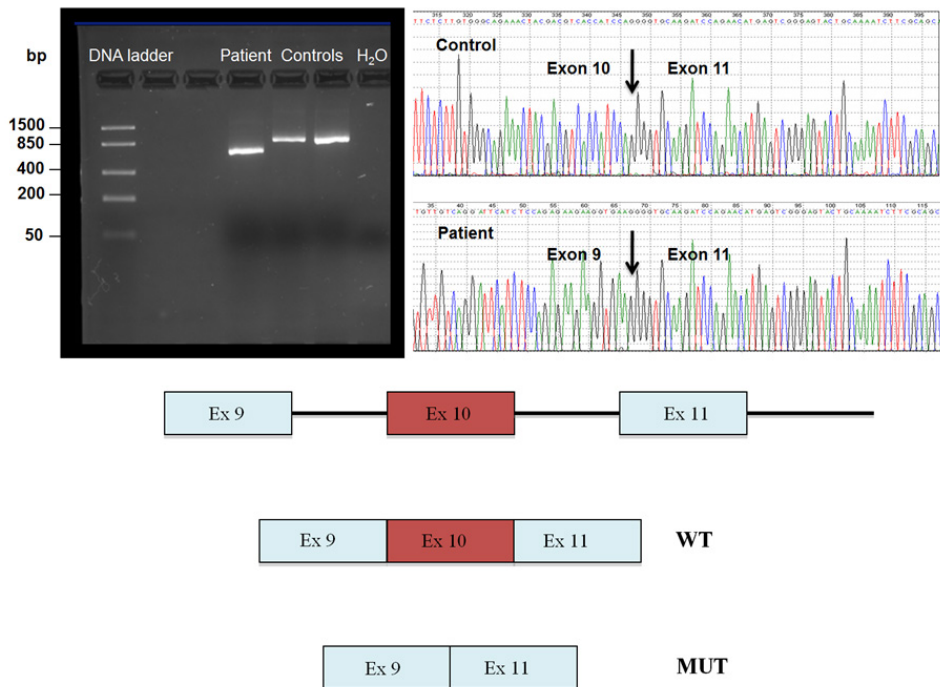
Supplemental Table 1. Primer sequences used for Sanger sequencing.

| Name | Forward primer |
|------------|----------------------------------|
| ALPK3_ex1A | 5'-GAAGTGTTAATTGAGCCCCCTAATCT-3' |
| ALPK3_ex1B | 5'-GCGCTACTGCAGACACCAG-3' |
| ALPK3_ex2 | 5'-ATGGAGCAGGCCAACTAAGAC-3' |
| ALPK3_ex3 | 5'-CAGGCATGGTAAGACGGAAG-3' |
| ALPK3_ex4 | 5'-GCCTCTTCCCATTATTTTGA-3' |
| ALPK3_ex5A | 5'-GTTGTATGTTGTGACGTGTGAGATG-3' |
| ALPK3_ex5B | 5'-ACCATGACTGAGTACAAGATCCAC-3' |
| ALPK3_ex5C | 5'-GCCTGACTCCTGTGGGACT-3' |
| ALPK3_ex6A | 5'-GGATGCCAGACTGGAAAGAG-3' |
| ALPK3_ex6B | 5'-ACACAGGAAGACAGAAGGATGC-3' |
| ALPK3_ex6C | 5'-GTATGGATCAGGGTGGCTGT-3' |
| ALPK3_ex6D | 5'-CTGCTGAGCCCCTGTACCT-3' |
| ALPK3_ex6E | 5'-CCCTCCCAAGAGGAGAAGTT-3' |
| ALPK3_ex7 | 5'-GCTTCTCTCTAGCTGAGATGTGTG-3' |
| ALPK3_ex8 | 5'-AGGACTGCAAACCAGACCTGT-3' |
| ALPK3_ex9 | 5'-GGCAGCAGTCATCTTTGAGAG-3' |
| ALPK3_ex10 | 5'-CCTTTTCTTCCCTGTGAGC-3' |
| ALPK3_ex11 | 5'-AGTCCCCTAACAGAATAGGTAGCC-3' |
| ALPK3_ex12 | 5'-GGCCCTTCTTTTAGGTCCAAG-3' |
| ALPK3_ex13 | 5'-GCAGGAAGAGACATGGTTCTAAGC-3' |
| ALPK3_ex14 | 5'-ATGTACCCTGAGCACGACATC-3' |

Supplemental Table 2. Whole exon sequence variant filtering.

| Filtering step | Family A | Family B |
|--------------------------------|----------|----------|
| Input variants | 32802 | 38784 |
| Read depth ≥ 6 | 31931 | 38261 |
| Exons and flanking sequences | 28040 | 28985 |
| Population frequency | 2463 | 2269 |
| Heterozygous in father | 1268 | 893 |
| Homozygous in patient | 60 | 133 |
| Effect on protein | 37 | 107 |
| Presence in homozygous regions | 1 | 8 |
| Overlapping genes | | 1 |

| Reverse primer | Amplicon size |
|-------------------------------|---------------|
| 5'-CGCGCCCCTATTTATAGCC-3' | 437 |
| 5'-CCCTCACAGGGACTGATCC-3' | 498 |
| 5'-GTTAGTGCACGAGCAGACACTC-3' | 279 |
| 5'-GTCACCTCACGTAGTTTTGTGC-3' | 335 |
| 5'-CAGACTGCTCCATTTCTGAGG-3' | 264 |
| 5'-CAGAAGCAAACTGTTGATCAGG-3' | 549 |
| 5'-GCTGGCTTCCTGGTACTATCTGT-3' | 659 |
| 5'-TGCAGCAAGAGTTCCATGA-3' | 668 |
| 5'-TGGTTCCTGGAGGCTGTAC-3' | 774 |
| 5'-CCAGTTCAGGAAGAGAAGG-3' | 548 |
| 5'-AGGGACAGTGAGGGAGCTG-3' | 671 |
| 5'-CTGCTCTGACCTTAGGGAGAAAT-3' | 433 |
| 5'-GTTAGCAGCAGCAGCAGTGT-3' | 483 |
| 5'-GAATAAAAGGACCTCCCCTGGT-3' | 485 |
| 5'-GCCTTCTCTCAAAGATGACTGC-3' | 387 |
| 5'-AAGGGTGAACCTAATCCTGTGC-3' | 338 |
| 5'-TACTGGGCATCCTAACAGGAC-3' | 444 |
| 5'-ATTTGTGAGGCCACTGAGC-3' | 343 |
| 5'-CACTATGGCTTTCCTCCTC-3' | 395 |
| 5'-GCATCAGTAATAGCTGCCACAC-3' | 360 |
| 5'-GCACCTTCTCCAGTTAGTTCCA-3' | 555 |



Supplemental Figure 1. Results of reverse transcriptase PCR analysis. To investigate the effect of the *ALPK3* c.4736-1G>A variant on RNA splicing, we designed a reverse transcriptase PCR experiment (RT-PCR) using RNA isolated from fibroblasts of patient A-IX:2 (cDNA forward primer sequence 5'-GTGCACCATCCACAATGAGC-3', cDNA reverse primer sequence 5'-GACTAGGGAGGCCTTCTTCTG-3'). Low range DNA ladder is used as size standard. Analysis of the resulting RT-PCR product, covering *ALPK3* exon 10 and flanking sequences in the wild-type situation, by 2% agarose gel electrophoresis showed a smaller product in the patient (\pm 630 nucleotides) compared to the controls (\pm 900 nucleotides). Subsequent Sanger sequencing of the respective RT-PCR products confirmed that the *ALPK3* c.4736-1G>A mutation leads to complete skipping of exon 10, which comprises 281 nucleotides.

Supplemental references

1. Hedley PL, Jorgensen P, Schlamowitz S, et al. The genetic basis of long QT and short QT syndromes: a mutation update. *Hum Mutat* 2009;30:1486-1511.
2. Li H, Durbin R. Fast and accurate long-read alignment with Burrows-Wheeler transform. *Bioinformatics* 2010;26:589-595.
3. Li H, Handsaker B, Wysoker A, et al. The Sequence Alignment/Map format and SAMtools. *Bioinformatics* 2009;25:2078-2079.
4. McKenna A, Hanna M, Banks E, et al. The Genome Analysis Toolkit: a MapReduce framework for analyzing next-generation DNA sequencing data. *Genome Res* 2010;20:1297-1303.

